The Canadian Mineralogist
Vol. 48, pp. 513-521 (2010)
DOI: 10.3749/canmin.48.3.513

THE HYDROTHERMAL RECRYSTALLIZATION OF METAMICT ALLANITE-(Ce)

ANDREA ČOBIĆ§, VLADIMIR BERMANEC AND NENAD TOMAŠIĆ

Institute of Mineralogy and Petrology, Faculty of Science, University of Zagreb, Horvatovac 95, HR–10000 Zagreb, Croatia

RADEK ŠKODA

Institute of Geological Science, Masaryk University, Kotlarska 2, 61137 Brno, Czech Republic

ABSTRACT

Samples of metamict allanite-(Ce) originating from granite pegmatites were recrystallized by heating in air and under hydrothermal conditions. Recrystallization in air resulted in partial recovery of the crystal structure at 650°C. Heating at higher temperatures resulted in decomposition of the allanite structure to a multiphase assemblage containing hematite, cerianite, feldspar, britholite and thorianite. To our knowledge, this is the first report of thorianite as a breakdown product of allanite in literature. The collapse of the structure is mainly related to the removal of structural H_2O. Recrystallization under hydrothermal conditions yielded a more rapid and complete recovery of the structure at lower temperatures, without the appearance of additional phases. The stability of the allanite structure during hydrothermal recrystallization is related to the retention of OH^- groups, available because of the aqueous environment of recrystallization. Also, H_2O promotes a more rapid and efficient recrystallization due to the enhanced diffusion of cations. Crystallite size and strain calculation also record evidence of the recovery of the structure of damaged allanite.

Keywords: allanite-(Ce), metamictization, hydrothermal recrystallization, X-ray diffraction, granitic pegmatites.

SOMMAIRE

Nous documentons la recristallisation de l'allanite-(Ce) prélevée de pegmatites granitiques par chauffage dans l'air et sous conditions hydrothermales. Dans l'air, la recristallisation permet de récupérer partiellement la structure à 650°C. Un chauffage à températures plus élevées mène à la déstabilisation de la structure pour donner un assemblage multiphasé contenant hématite, cérianite, feldspath, britholite et thorianite. A notre connaissance, ce serait la première fois que la thorianite figure parmi les produits de déstabilisation de l'allanite. La destruction de la structure est surtout liée à l'élimination de H_2O comme composant structural. Un traitement hydrothermal mène à une recristallisation plus rapide et plus complète de la structure, et à des températures plus faibles, sans formation de phases additionnelles. La stabilité de la structure de l'allanite-(Ce) au cours de la recristallisation hydrothermale est liée à la préservation des groupes OH^- dans la structure, résultat du milieu aqueux de la recristallisation. Aussi, la présence de H_2O favorise une transformation plus rapide et efficace à cause de son rôle à faciliter la difusion des cations. La taille des domaines cristallins et l'importance de déformation démontrent aussi le progrès de la recristallisation structurale de l'allanite endommagée.

(Traduit par la Rédaction)

Mots-clés: allanite-(Ce), métamictisation, recristallisation hydrothermale, diffraction X, pegmatites granitiques.

INTRODUCTION

Allanite, which belongs to the epidote group, has the general formula $A_2M_3[T_2O_7|TO_4](O,F)(OH,O)$, with A = Ca, REE, Mn, Fe^{2+}, Pb, Sr, Th and U, M = Al, Fe^{2+}, Fe^{2+}, Mn^{2+}, Mn^{3+}, Ti and Mg, and T = Si, Al (Deer *et al.* 1986, Armbruster *et al.* 2006). Allanite is commonly metamict. The metamict state of allanite and other metamict minerals have been investigated extensively (Ewing 1987, 1994, Janeczek & Eby 1993) in order to explain the mechanisms of amorphization as well as to reconstitute the original crystal-structure. The recovery of the crystal structure is usually carried out by heating minerals in a controlled or uncontrolled atmosphere.

The majority of metamict minerals recrystallize at temperatures greater than 600°C. The recrystallization

§ *E-mail address*: ancobic@geol.pmf.hr

of allanite is complicated by the presence of structurally bound hydroxyl groups, which escape during recrystallization induced by heating. Also, in an uncontrolled atmosphere, Fe^{2+} can oxidize to Fe^{3+}. This inevitably results in decomposition of the allanite to more simple oxides and silicates (Berman 1955). In order to prevent these problems, hydrothermal recrystallization offers a reasonable approach to recrystallize those minerals containing structural water. Janeczek & Eby (1993) reported on the successful hydrothermal recrystallization of gadolinite, a mineral that does not contain H_2O in its structure. In the current study, this approach will be applied to allanite-(Ce) from granitic pegmatites sampled in Bulgaria, Mexico, two localities in Norway and three in Canada.

Background Information

Metamictization is usually attributed to α-decay of radionuclides, and a destructive impact of α-particles and α-recoil nuclei to the structure of minerals (Ewing 1994, Weber *et al*. 1998). Many minerals that contain radionuclides exhibit radiation damage to their crystal structures. However, there are minerals with a relatively high amount of radionuclides that do not show properties of metamict minerals, for instance apatite and monazite. In contrast, there are minerals that contain relatively low amount of radionuclides, but are metamict, *e.g.*, minerals of the allanite group.

Apart from the leading role of radionuclides in the metamictization of minerals, Graham & Thornber (1974) proposed that chemical composition and complexity of the crystal structure can be significantly responsible for metamictization. We thus suggest that chemical complexity (particularly of Nb–Ta oxides) due to substitution of a large number of highly charged cations with different ionic radii could lead to disproportionation and segregation to microregions and domains of different compositions and structure.

TABLE 1. DESCRIPTION OF THE ALLANITE SAMPLES INVESTIGATED

Sample	Locality	Host rock	
BG	Rila, Bulgaria	Granitic pegmatite	(1)
CDN1	Beryl Pit, Quadeville, Ontario, Canada	Granitic pegmatite	(2, 3)
CDN2	Wilson's Corners, McGregor Lake, Ontario, Canada	Granitic pegmatite	
CDN3	Older Township, Frontenac County, Ontario, Canada	Granitic pegmatite	(3)
MEX1	El Muerto mine, Oaxaca, Mexico	Granitic pegmatite	(4, 5)
MEX2*	El Muerto mine, Oaxaca, Mexico	Granitic pegmatite	(4, 5)
N1	Fone, Gjerstad, Aust-Agder, Norway	Granitic pegmatite	(6)
N2	Gloserheia, Froland, Aust-Agder, Norway	Granitic pegmatite	(7)

Note that sample MEX2 consists of rare-earth-enriched epidote rather than allanite-(Ce). References: (1) Alexandrov *et al.* (2001), (2) McEachern & van Breemen (1993), (3) Mezger *et al.* (1993), (4) Panczer (1987), (5) Melgarejo & Prol-Ledesma (1999), (6) Bjorlykke (1939), (7) Åmli (1975).

Experimental

The samples of allanite were examined using a stereomicroscope in order to remove visible impurities. The purified sample portions were used for further examinations. The origin of the samples is described in Table 1.

Prior to X-ray powder-diffraction analysis, the samples were ground in an agate mortar. X-ray powder-diffraction data were collected using a Philips PW 3040/60 X'Pert PRO diffractometer with a Cu tube used at 45 kV and at a current of 40 mA. The step size was 0.02° and the counting time was 2 s per step. Analyses of the X-ray-diffraction patterns and calculations of crystallite size and strain were performed using High-Score Plus software (Panalytical 2004). The unit-cell parameters were calculated using Unit Cell (Holland & Redfern 1997).

The chemical composition of natural samples was established using both energy-dispersive (EDS) and wavelength-dispersive systems (WDS). An Oxford Instruments EDS controlled by an INCA 250 system is mounted onto a scanning electron microscope Tescan Vega TS5136 MM used for qualitative analysis. A beam voltage of 20 kV and current of 10 nA were applied.

Quantitative chemical analyses were made with a CAMECA SX100 electron microprobe in the WDS mode at the following conditions: acceleration voltage 15 keV, beam current 20 nA, and beam diameter 2 μm. For quantification, the following standards were used: sanidine (Si and Al), albite (Na), andradite (Ca and Fe), Mg_2AlO_4 (Mg), spessartine (Mn), titanite (Ti), $ScVO_4$ (Sc), fluorapatite (P), $CeAl_2$ (Ce), LaB_6 (La), YAG (Y), a set of REE fluorides (Nd, Sm, Pr), $GdPO_4$ (Gd), $DyPO_4$ (Dy), Th (Th) and topaz (F). The abundances of K, U, Er, Yb and Zr are present below detection limits. Detection limits for the elements sought (in ppm) are: Si 440, Al 385, Na 569, K 344, Ca 576, Fe 920, Mg 278, Mn 578, Ti 342, Sc 257, P 222, Ce 861, La 836, Y 446, Nd 1735, Sm 767, Pr 1624, Gd 1179, Dy 1623, Er 700, Yb 1102, Th 1027, U 612, F 491 and Zr 415.

All samples were heated at 650 and 1000°C for 24 h in air. Samples MEX1 and MEX2 were also hydrothermally treated in a microwave oven Microwave Anton Paar 3000 (rotor 16HF – 100). A cuvette with 500 mg of the sample was filled up with water and heated to 200°C over 20 minutes. For the next 20 minutes, the temperature was maintained between 200 and 260°C. Afterward, the temperature was decreased to room temperature over 15 minutes.

Samples MEX2, CDN2, CDN3 and N1 were in addition treated in a Perkin–Elmer autoclave. The samples were heated in a Teflon vessel together with 5 mL of

water for each 200 mg of the sample. The vessel was enclosed in an aluminum housing and heated at 150°C on a hot plate for 2, 5 and 24 h. Details of the sample thermal treatment are presented in Table 2.

Results

X-ray-diffraction data

X-ray diffraction patterns of all unheated samples are characterized by a high background and broad diffraction-lines of low intensity. All observed diffraction-lines belong to allanite. Annealing the samples in air at 650°C for 24 h intensifies the diffraction lines and decreases their width. At the same time, a few additional diffraction-lines of allanite appear, which were not observed at room temperature.

As a result of heating at 1000°C, the crystal structure of allanite is destroyed, giving rise to simple oxides like hematite, cerianite and thorianite, and silicates like feldspar and britholite. The occurrence of these phases had been previously observed in the recrystallization of allanite (Lima-de-Faria 1958, Mitchell 1966, Vance & Routcliffe 1976, Janeczek & Eby 1993) with the exception of thorianite, probably due to problems in identification due to its low concentration in the resulting multiphase system. The products of heating of a representative sample of allanite, MEX1, annealed at 650 and 1000°C, are presented in Figure 1.

The sample hydrothermally treated at 150°C in an autoclave for 5 h shows more pronounced diffraction lines and a lower background than the sample treated the same way for 2 h (Fig. 2). On the other hand, the sample hydrothermally treated for 24 h but at lower temperature (130°C) yields less pronounced diffraction lines than either of the previously mentioned samples. Diffraction lines of all three samples all belong to allanite, without the appearance of any other phases. This is also true for the samples hydrothermally treated in a microwave oven (Fig. 2). There is no large difference among the samples treated in autoclave and those treated in a microwave oven except for a slight difference in intensity and resolution of diffraction lines, which is probably due to a difference in duration of the hydrothermal treatment. The unit-cell calculations show increasing crystallinity (Table 3). The results of a crystallite size and strain analysis are presented in Table 4.

TABLE 2. THERMAL TREATMENT OF THE ALLANITE SAMPLES

Sample		Annealing temperature (°C)	Hydrothermal treatment T (°C)	Treatment duration (h)
BG	BG_RT	–	–	–
	BG_650	650	–	24
	BG_1000	1000	–	24
CDN1	CDN1_RT	–	–	–
	CDN1_650	650	–	24
	CDN1_1000	1000	–	24
CDN2	CDN2_RT	–	–	–
	CDN2_650	650	–	24
	CDN2_1000	1000	–	24
	CDN2_AK_1		140–150	2
	CDN2_AK_2		150	5
	CDN2_AK_3		150	24
	CDN2_AK_4		130	24
CDN3	CDN3_RT	–	–	–
	CDN3_650	650	–	24
	CDN3_1000	1000	–	24
	CDN3_AK_1		140–150	2
	CDN3_AK_2		150	5
	CDN3_AK_3		150	24
MEX1	MEX1_RT	–	–	–
	MEX1_650	650	–	24
	MEX1_1000	1000	–	24
	MEX1_MD		200–260	0.3
MEX2	MEX2_RT	–	–	–
	MEX2_650	650	–	24
	MEX2_1000	1000	–	24
	MEX2_AK_1		140–150	2
	MEX2_AK_2		140–150	5
	MEX2_AK_3		150	24
	MEX2_MD_1		200–260	0.3
N1	N1_RT	–	–	–
	N1_400	400	–	24
	N1_500	500	–	24
	N1_650	650	–	24
	N1_800	800	–	24
	N1_1000	1000	–	24
	N1_AK_1	–	150	2
	N1_AK_2	–	150	5
	N1_AK_3	–	150	24
N2	N2_RT	–	–	–
	N2_500	500	–	24
	N2_650	650	–	24
	N2_800	800	–	24
	N2_1000	1000	–	24

Chemical composition

Both WDS and EDS analyses show evidence of heterogeneity of the natural samples investigated. Most of the analyzed spots depict compositions in the range $Aln_{0.25}Ep_{0.75}$ – $Aln_{0.89}Ep_{0.11}$. The most abundant REE in all the samples is Ce, followed by La (Table 5). The actinide content is slightly above or below 1%, mainly due to ThO_2, whereas uranium is below the detection limit. The sum of REE + Th in all the samples is >0.5 *apfu*, except in sample MEX2; thus the investigated samples belong to the subgroup allanite (Armbruster *et al.* 2006). Sample MEX2, with the calculated formula $(Ca_{0.97}Mn_{0.03})_{\Sigma 1.00}(Ca_{0.70}REE_{0.27}Th_{0.02})_{\Sigma 0.99}(Al_{0.96}Fe^{3+}{}_{0.02})_{\Sigma 0.98}Al(Fe^{2+}{}_{0.85}Mg_{0.03}Fe^{3+}{}_{0.12})_{\Sigma 1.00}[Si_{1.03}O_4|Si_2O_7]O(OH_{0.77}O_{0.23})$, is a solid solution between epidote (dominant) and allanite.

Formula calculations for all natural samples of allanite were performed in agreement with the recommended nomenclature of epidote-group minerals (Armbruster *et al.* 2006). Normalization of electron-microprobe data was done on the basis of $\Sigma(A + M + T)$

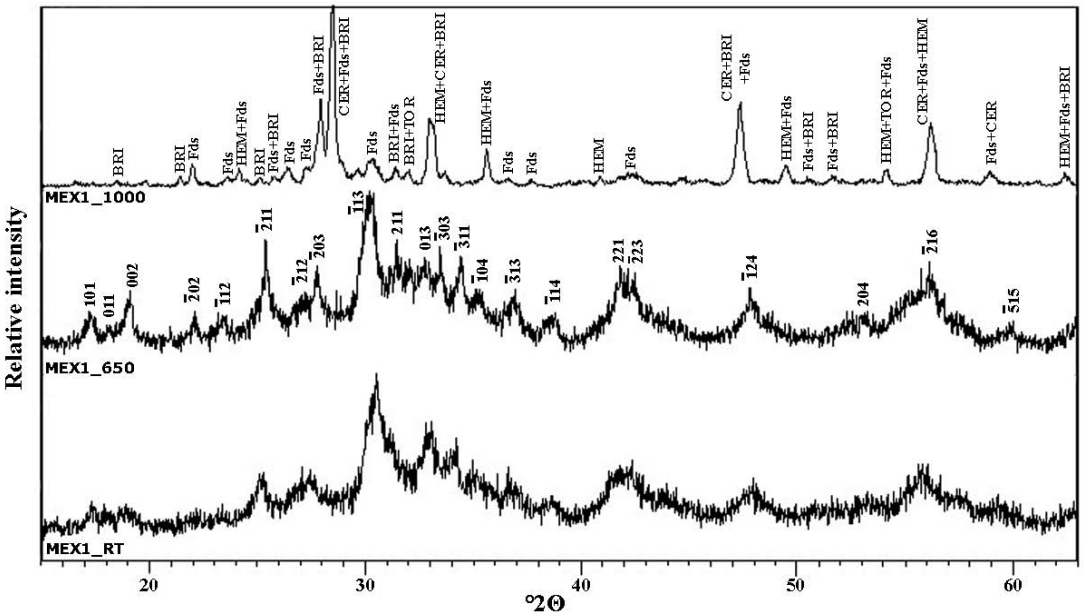

FIG. 1. XRD patterns of allanite sample MEX1 at room temperature, 650 and 1000°C (BRI: britholite, Fds: feldspar, HEM: hematite, CER: cerianite, TOR: thorianite).

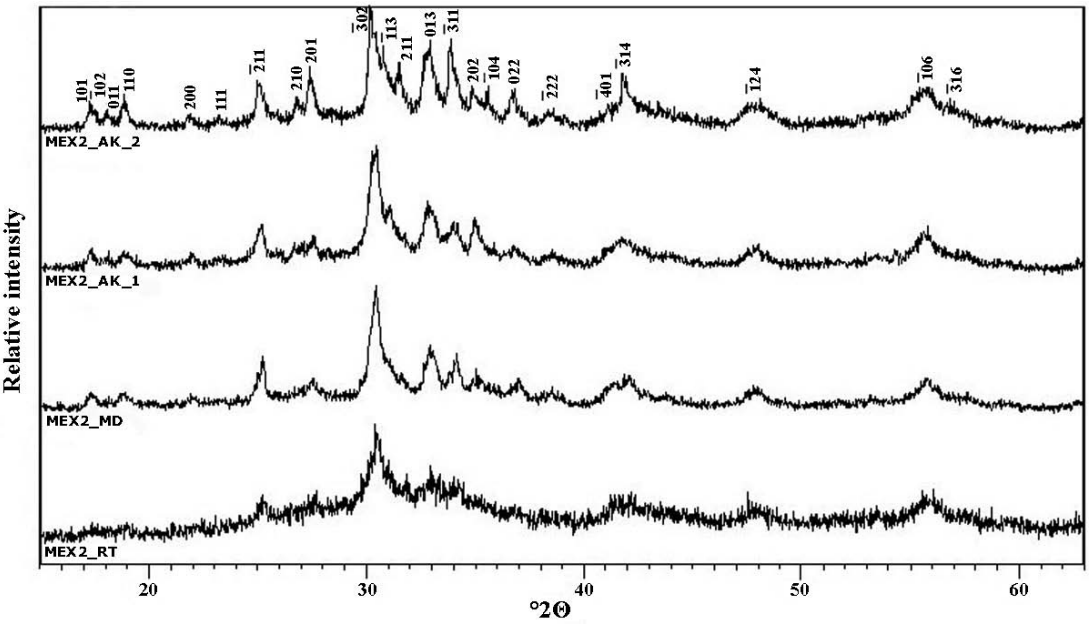

FIG. 2. XRD patterns of sample MEX2 at room temperature (MEX2_RT) and heated in a microwave digestor (MEX2_MD) at 200–260°C for 20 minutes and in an autoclave at 150°C for 2 (MEX2_AK_1) and 5 h (MEX2_AK_2).

= 8 *apfu*. The content of Fe determined by EMPA was initially assumed to be Fe^{2+}. However, this resulted in an excess of oxygen in formula calculation, which was assigned to Fe^{3+} in the allanite samples. The recalculated formulae thus contain both Fe^{2+} and Fe^{3+}.

As observed in back-scattered electron (BSE) images, the samples investigated belong to a paragenesis with other minerals that occur as nests, lamellae and veinlets in allanite (Fig. 3). Along with lamellae of epidote enriched in REE, other silicates like thorite (Table 6) occur in some samples (Figs. 3a, b, c). Also, xenotime-(Y) (Fig. 3b, Table 7), veinlets of REE carbonate, most likely bastnäsite-(Ce), and calcium carbonate (Fig. 3a) are observed.

TABLE 3. UNIT-CELL PARAMETERS OF THE SAMPLES, INVESTIGATED AT DIFFERENT TEMPERATURES OF RECRYSTALLIZATION

Sample	*a* (Å)	*b* (Å)	*c* (Å)	β (°)	*V* (Å^3)
BG_RT	8.960(7)	5.736(4)	10.189(7)	114.87(5)	475.1(4)
BG_650	8.978(7)	5.737(3)	10.215(5)	115.12(5)	476.3(3)
CDN2_RT	8.99(1)	5.761(5)	10.279(6)	114.94(8)	482.8(4)
CDN2_650	8.960(9)	5.68(1)	10.27(1)	114.78(9)	476.7(8)
CDN2_AK_1	9.005(9)	5.768(6)	10.30(1)	114.93(9)	485.2(6)
CDN2_AK_2	8.99(2)	5.726(7)	10.29(1)	115.2(1)	479.6(8)
CDN2_AK_3	8.96(2)	5.72(2)	10.25(2)	114.8(2)	477(2)
CDN3_RT	8.959(5)	5.756(4)	10.225(5)	115.24(7)	476.9(4)
CDN3_650	8.940(3)	5.697(3)	10.326(6)	115.61(3)	474.3(2)
CDN3_AK_1	8.961(9)	5.743(5)	10.215(5)	115.12(8)	476.0(4)
CDN3_AK_2	8.969(3)	5.758(2)	10.231(4)	115.29(3)	477.7(2)
MEX1_RT	8.99(2)	5.72(2)	10.26(2)	115.4(2)	476.4(9)
MEX1_650	8.94(3)	5.73(2)	10.27(2)	115.0(3)	477(2)
MEX1_MD_1	8.982(9)	5.738(9)	10.193(9)	115.03(7)	476.0(5)
MEX2_RT	8.957(8)	5.738(8)	10.35(1)	114.90(8)	482.6(7)
MEX2_650	8.987(7)	5.709(9)	10.23(1)	114.92(5)	476.1(6)
MEX2_AK_1	9.003(4)	5.751(4)	10.258(9)	115.26(6)	480.4(3)
MEX2_AK_2	8.983(6)	5.757(4)	10.215(9)	115.11(6)	478.3(4)
MEX2_MD_1	8.968(6)	5.733(8)	10.25(1)	115.46(6)	475.8(5)
N1_650	8.955(3)	5.718(2)	10.325(5)	115.41(3)	477.5(2)
N1_800	8.984(7)	5.716(6)	10.205(7)	115.03(6)	474.8(4)
N2_RT	9.03(2)	5.762(6)	10.24(2)	115.1(2)	483(1)
N2_500	8.91(2)	5.74(1)	10.24(2)	114.9(1)	475(1)
N2_650	9.01(1)	5.74(1)	10.231(6)	114.84(8)	480(1)
N2_800	8.999(6)	5.735(6)	10.284(5)	114.83(5)	481.7(4)

TABLE 4. CRYSTALLITE SIZE AND STRAIN PARAMETERS CALCULATED FOR SAMPLE MEX2

Sample	Crystallite size (Å)	Strain (%)
MEX2_RT	74.6	0.590
MEX2_AK_1	94.1	0.479
MEX2_AK_2	167.1	0.489

DISCUSSION

The samples of allanite that we chose for study are metamict. The chemical analysis confirmed the presence of allanite with a complex composition and with

TABLE 5. CHEMICAL COMPOSITION OF THE SAMPLES OF ALLANITE-(Ce) INVESTIGATED

sample	BG	CDN1	CDN2	CDN3	MEX1	MEX2*	N1	N2
SiO_2 wt.%	31.32	30.55	30.48	30.21	30.65	34.43	30.09	30.43
Al_2O_3	17.56	13.82	16.54	11.26	15.66	18.91	11.34	14.63
FeO	8.89	10.08	3.51	11.21	9.12	11.53	13.80	10.51
Fe_2O_3	3.82	4.15	6.72	4.29	5.57	2.12	3.62	3.38
CaO	12.67	11.32	10.64	9.53	9.50	17.73	9.45	11.42
Na_2O	<0.06	0.18	<0.06	0.36	<0.06	<0.06	<0.06	0.19
MgO	0.96	0.19	1.98	<0.03	<0.03	0.26	0.64	0.53
MnO	0.35	0.66	0.55	0.70	0.47	0.44	0.22	0.40
TiO_2	0.26	0.41	0.31	0.67	0.55	<0.03	1.06	0.31
Sc_2O_3	<0.03	<0.03	<0.03	<0.03	<0.03	<0.03	<0.03	0.41
P_2O_5	<0.02	<0.02	0.88	<0.02	<0.02	<0.02	<0.02	<0.02
Ce_2O_3	9.36	9.76	10.17	11.49	11.87	3.41	10.19	5.98
La_2O_3	5.38	6.27	6.54	8.87	5.61	1.64	7.66	2.40
Y_2O_3	<0.05	0.14	<0.05	<0.05	0.31	0.70	<0.05	1.86
Nd_2O_3	2.80	2.05	2.12	1.70	3.82	1.39	1.72	4.50
Sm_2O_3	0.40	0.27	0.22	<0.08	0.57	0.38	0.16	1.63
Pr_2O_3	0.95	0.68	0.89	0.73	1.04	0.40	0.69	0.88
Gd_2O_3	<0.12	<0.12	<0.12	<0.12	<0.12	<0.12	<0.12	1.23
Dy_2O_3	<0.16	<0.16	<0.16	<0.16	<0.16	<0.16	<0.16	0.42
ThO_2	0.77	0.95	0.61	0.64	0.86	1.23	1.22	1.52
F	0.20	0.45	0.71	0.46	0.29	<0.05	0.23	0.12
O=F	0.08	0.19	0.30	0.19	0.12	<0.02	0.10	0.05
Total	95.47	91.46	92.05	91.66	95.60	94.56	91.85	92.63
Si *apfu*	2.95	3.08	3.01	3.16	3.04	3.03	3.10	3.01
Al	0.05	–	–	–	–	–	–	–
Σ *T*	3.00	3.08	3.01	3.16	3.04	3.03	3.10	3.01
Al	1.90	1.64	1.91	1.39	1.83	1.96	1.38	1.71
Fe^{2+}	0.67	0.85	0.20	0.98	0.71	0.85	1.16	0.87
Fe^{3+}*	0.27	0.32	0.50	0.34	0.42	0.14	0.28	0.25
Mg	0.14	0.03	0.29	–	–	0.03	0.10	0.08
Mn	–	0.06	–	0.06	–	0.02	–	0.03
Ti	0.02	0.03	0.02	0.05	0.04	–	0.08	0.02
Sc	–	–	–	–	–	–	–	0.04
P	–	–	0.07	–	–	–	–	–
Σ *M*	3.00	2.93	3.00	2.82	3.00	3.00	3.00	3.00
Ca	1.28	1.22	1.12	1.07	1.01	1.67	1.04	1.21
Na	–	0.04	–	0.07	–	–	–	0.04
Fe^{2+}	0.03	–	0.09	–	0.05	–	0.03	–
Mn	0.03	–	0.05	–	0.04	0.02	0.02	–
Ce	0.32	0.36	0.37	0.44	0.43	0.11	0.38	0.22
La	0.19	0.23	0.24	0.34	0.21	0.05	0.29	0.09
Y	–	0.01	–	–	0.02	0.03	–	0.10
Nd	0.09	0.07	0.07	0.06	0.14	0.04	0.06	0.16
Sm	0.01	0.01	0.01	–	0.02	0.01	0.01	0.06
Pr	0.03	0.02	0.03	0.03	0.04	0.01	0.03	0.03
Gd	–	–	–	–	–	–	–	0.04
Dy	–	–	–	–	–	–	–	0.01
Th	0.02	0.02	0.01	0.02	0.02	0.02	0.03	0.03
Σ *A*	2.00	1.99	1.99	2.03	1.96	1.97	1.90	1.99
REE+Th	0.67	0.73	0.73	0.89	0.86	0.29	0.80	0.74
Ce/La	1.72	1.56	1.44	1.29	2.00	1.93	1.33	2.61
F	0.06	0.14	0.22	0.15	0.09	–	0.08	0.04

* The amount of Fe^{3+} is calculated. The formulae are calculated on the basis of Σ(*A* + *M* + *T*) = 8 *apfu*. Sample MEX-2 consists of rare-earth-enriched epidote-(Ce) rather than allanite-(Ce).

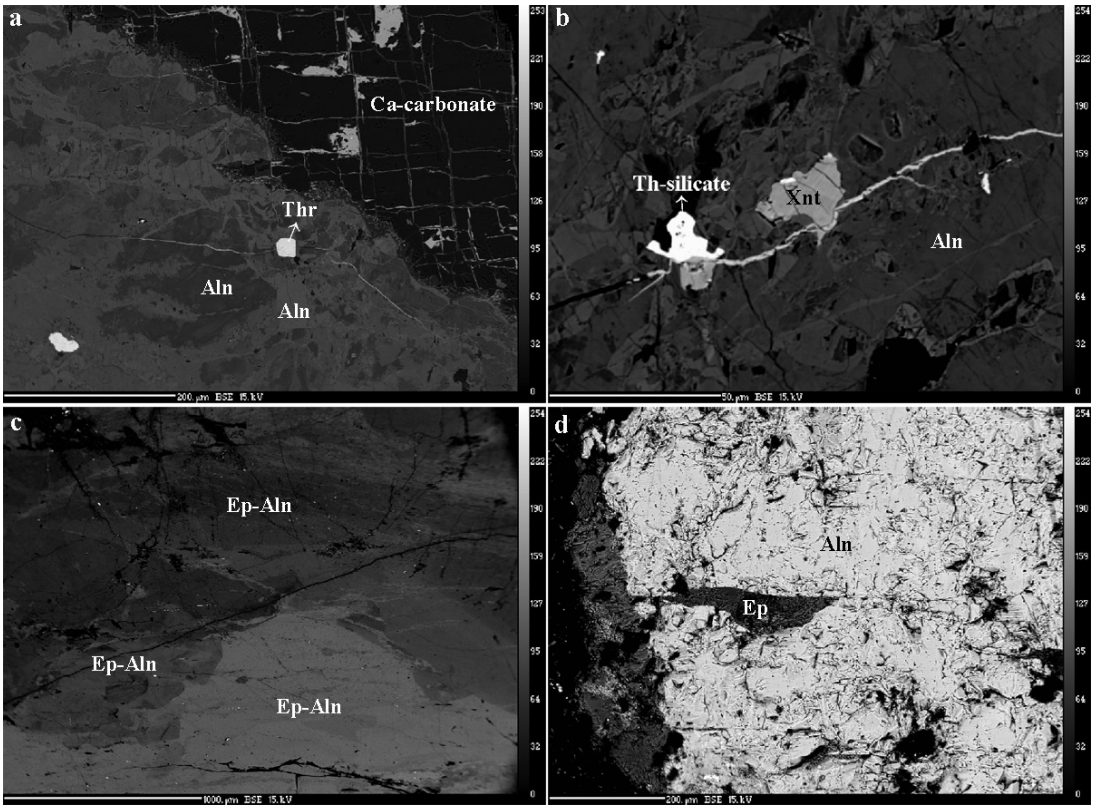

FIG. 3. (a) Sample N2, several generations of allanite with islands of thorite; (b) sample N2: Th silicate and xenotime-(Y), (c) sample MEX2: several generations of allanite–epidote series with various compositions; the white spots represent a Th silicate (thorite or huttonite); (d) BG: lamellae of epidote in allanite.

TABLE 6. CHEMICAL COMPOSITION AND CALCULATED FORMULA OF THORITE IN SAMPLES N1 AND N2

sample	N1	N2		N1	N2
ThO_2 wt.%	70.44	58.00	Th *apfu*	0.90	0.67
UO_2	3.88	5.88	U	0.05	0.07
SiO_2	17.75	19.84	Si	1.00	1.00
Al_2O_3	0.14	0.74	Al	0.01	0.04
PbO	1.65	0.60	Pb	0.02	0.01
Y_2O_3	0.33	1.01	Y	0.01	0.03
CaO	1.45	2.42	Ca	0.09	0.13
FeO	1.27	1.81	Fe^{2+}	0.06	0.08
As_2O_5	0.16	<0.08	As	–	–
P_2O_5	<0.05	0.31	P	–	0.01
Total	97.07	90.62	Σ cations	2.15	2.03

The formulae are calculated on the basis of Si = 1 *apfu*.

TABLE 7. CHEMICAL COMPOSITION AND CALCULATED FORMULA OF XENOTIME-(Y) IN SAMPLE N2

Y_2O_3 wt.%	40.97	Y *apfu*	0.74
P_2O_5	32.73	P	0.94
SiO_2	1.36	Si	0.05
Al_2O_3	0.38	Al	0.01
CaO	0.13	Ca	–
FeO	2.12	Fe	0.06
PbO	0.29	Pb	–
ThO_2	0.19	Th	–
REE_2O_3	16.60	ΣREE	0.92
As_2O_5	0.74	As	0.01
Total	95.49	Σ cations	2.00

The formula is calculated on the basis of Σ(P + Si + Al + As) = 1 *apfu*.

a large number of cations having different ionic radii and charges (Th, Na, Mg, Mn, REE). The difference in ionic radius and charge of many different cations in a complex crystal structure favors metamictization (Wang *et al*. 1991).

Radionuclides play a significant role in metamictization; α decay of the radionuclides present in the

mineral structure is considered to be the main reason for metamictization (Ewing 1994, Weber *et al*. 1998). In all the samples, radionuclides are present, mainly Th (Table 5). By thorough analysis of XRD patterns, we found that sample N1 shows the highest degree of metamictization, which corresponds well with a significant content of Th (Fig. 4).

The recrystallization of metamict minerals containing structural H_2O is complicated by the escape of H_2O in routine recrystallization experiments in air (Bonazzi & Menchetti 1994). The removal of structural H_2O from allanite, *i.e*., OH^- groups, is favored by a simultaneous oxidation of divalent cations in octahedral positions (Bonazzi & Menchetti 1994). The charge balance is maintained by H^+ removal during oxidation of, for instance, Fe^{2+} and Mn^{2+}. This reaction can be described by equation

$$2OH^- - e^- \rightarrow H_2O + \tfrac{1}{2}\, O_2,$$

which liberates oxygen for the oxidation of iron and the balancing of charges described by following equation:

$$2Fe^{2+} + \tfrac{1}{2}\, O_2 \rightarrow 2Fe^{3+} + O^{2-}.$$

However, the recrystallization in this case is limited by dehydroxylation and consequent destruction of the crystal structure. Thus, allanite is decomposed to hematite, cerianite, feldspar, britholite and thorianite. The samples that are less strongly metamict are more easily recrystallized (Janeczek & Eby 1993) because they contain more relics of the original structure. Indeed, the recrystallization at 650°C in air showed that the samples with a lower degree of metamictization are more readily recrystallized. The preserved relics of the original structure serve as centers of epitactic recrystallization (Tomašić *et al*. 2006). The recrystallization is also accompanied by a decrease in unit-cell volume, as has been demonstrated in a previous investigation by Janeczek & Eby (1993), who showed that the volume of unit-cell increases during metamictization and decreases as the mineral recrystallizes (Table 3).

During the recrystallization of allanite in air at temperatures around 1000°C, new phases appear, mainly silicates and simple oxides. Thus, silicates like feldspars (Lima-de-Faria 1958) or britholite (Mitchell 1966, Janeczek & Eby 1993) have been observed. Heating experiments in an oxidizing atmosphere yield oxides like cerianite and hematite (Vance & Routcliffe 1976). Unlike previous studies, thorianite was also observed in our investigation.

Owing to the problems arising in recrystallization experiments of OH-containing minerals in air, it is more appropriate to recover crystal structures hydrothermally. In this way, H_2O is preserved in its positions in the crystal structure. A study of anhydrous gadolinite (Janeczek & Eby 1993) showed that hydrothermal heating results in a direct recrystallization of gadolinite without an occurrence of other phases. Moreover, recrystallization of metamict zircon in hydrothermal

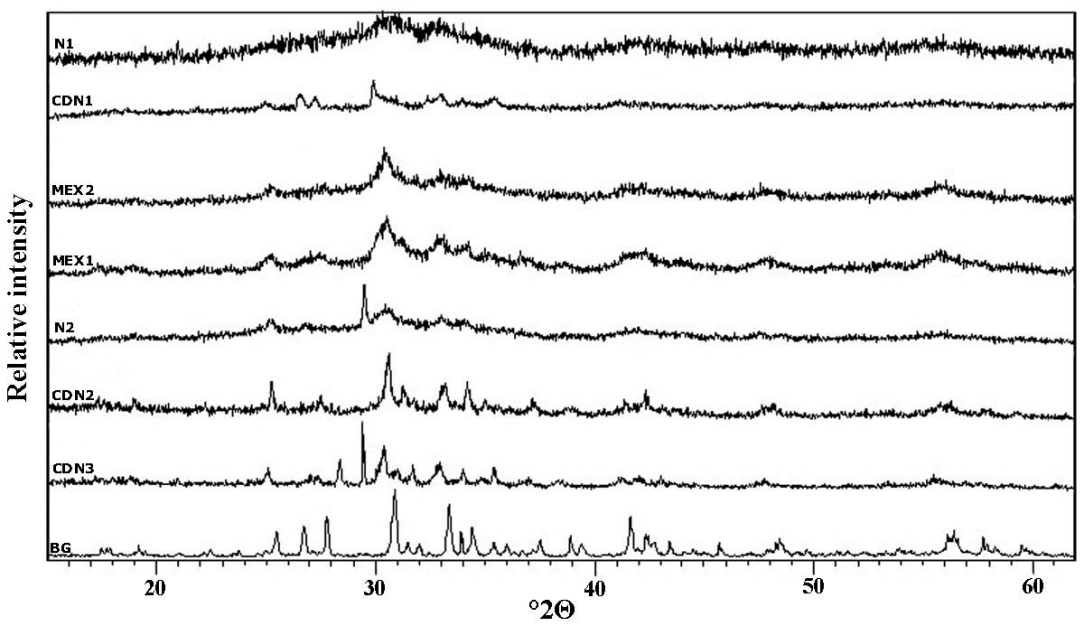

FIG. 4. XRD patterns of the allanite samples investigated at room temperature.

conditions showed that H_2O can play the role of a catalyst in crystal-structure recovery (Geisler *et al*. 2003). Our XRD patterns of allanite hydrothermally treated in a microwave oven and autoclave show partial but nevertheless significant recrystallization. The temperatures and pressures applied are relatively low, but recrystallization occurs quickly, yielding no additional phases.

Recrystallization is also made evident by changes in crystallite size and strain parameters. In the case of hydrothermally recrystallized samples, the crystallite size increases, whereas strain decreases. After 24 h of recrystallization, there is an indication of oxidation of Fe and Ce, probably inhibiting further recrystallization. This is based on the observed increase in strain and decrease in the *b* parameter (Tables 4, 3).

Our chemical analyses show that Ce is the dominant REE in the samples investigated. In addition to Th, which resides in the crystal structure, our SEM investigation confirmed the occurrence of thorite (Table 6) in a form of veinlets and grains intergrown with allanite. The distribution of Th indicates the development of thorite nuclei.

Bonazzi & Menchetti (1995) showed that the unit-cell parameter *b* is strongly related to the ionic radius of cations in octahedral coordination in the structure of epidote-group minerals. With an increase of Fe^{2+} content, an increase in the *b* parameter also occurs, and iron oxidation causes its decrease as well as the decrease of *a* and β parameters (Bonazzi & Mencheti 1994). The decrease in the *b* parameter in the case of allanite samples investigated thus suggests Fe oxidation. On the other hand, the increase in the *c* parameter can be related to a release of H^+, *i.e.*, H_2O (Table 3) (Bonazzi & Menchetti 1995), a result of the heating experiments being performed in an uncontrolled atmosphere. Structure recovery upon heating is also indicated by a decrease in unit-cell volume. Although these general relations in the behavior of unit-cell parameters are applicable to the majority of our allanite samples, some discrepancies can be observed due to the complex chemical composition, various degrees of metamictization, possible alteration and oxidation.

Conclusions

All of the investigated samples but one consist of allanite-(Ce), as confirmed by chemical analysis. Inclusions of Th phases like $ThSiO_4$ are found. A comparison of X-ray-diffraction data shows that the degree of metamictization is related to the content of radionuclides in the structure of the investigated samples. Also, severely metamict samples contain larger amount of REE. Significant contents of large cations with different ionic radii and charges indicate that the degree of metamictization is favored by crystal structure instabilities caused by a complex chemical composition (and structure).

The recrystallization experiments were performed dry (in air) and in aqueous (hydrothermal) environments. Partial recovery of the structure at 650°C in air is followed by a collapse of the structure at higher temperatures accompanied by an occurrence of phases like hematite, cerianite, thorianite, feldspar and brithollite. The collapse of the structure is mainly associated with the removal of OH^- groups from the structure, but also with oxidation of Fe and Ce. On the other hand, hydrothermal recrystallization occurs more quickly and at lower temperatures compared to dry recrystallization in air. There is no indication of mineral decomposition during a prolonged hydrothermal treatment. Crystallite size and strain analysis indicate a fast and significant recovery of the structure at low temperatures and pressures. The results of hydrothermal recrystallization suggest that H_2O in the system enables a more rapid diffusion of ions in the structure at lower temperature, and thus promotes recovery of the structure. Recrystallization in an aqueous environment also enables H_2O retention in the structure, which is crucial for its preservation.

Recrystallization experiments in air are indicated by unit-cell parameters behavior: both unit-cell volume and the parameter *b* decrease during recrystallization, thus giving evidence of structural recovery and possible oxidation of Fe^{2+}, respectively. During dry recrystallization, the *c* parameter increases, as a result of the removal of OH^- group from the crystal structure. Hydrothermal recrystallization yielded an even more significant decrease of the unit-cell volume, which indicates a more rapid rate of recrystallization.

Acknowledgements

The authors are grateful to the Ministry of Science, Education and Sport of the Republic of Croatia for supporting this work (grants No 119–0000000–1158, 098–0982934–2742). Grant GAAV no. KJB301630801 of the Czech Republic was awarded to R. Škoda. We thank Goran Durn, from RGNF, who supported this investigation with his autoclave. The authors also thank the reviewers, Greg Lumpkin and Lee Groat, and Michael Easton (Ontario Geological Survey) and Robert Linnen, for their constructive help and useful suggestions.

References

Alexandrov, P., Guiliani, G. & Zimmerman, J.-L. (2001): Mineralogy, age, and fluid geochemistry of the Rila emerald deposits, Bulgaria. *Econ. Geol.* **96**, 1469-1476.

Åmli, R. (1975): Mineralogy and rare earth geochemistry of apatite and xenotime from the Gloserheia granite pegmatite, Froland, Southern Norway. *Am. Mineral.* **60**, 607-620.

Armbruster, T., Bonazzi, P., Akasaka, M., Bermanec, V., Chopin, C., Gieré, R., Heuss-Assbichler, S., Liebscher,

A., MENCHETTI, S., PAN, YUANMING & PASERO, M. (2006): Recommended nomenclature of epidote-group minerals. *Eur. J. Mineral.* **18**, 551-567.

BERMAN, J. (1955): Identification of metamict minerals by X-ray diffraction. *Am. Mineral.* **40**, 805-827.

BJORLYKKE, H. (1939): Feltspat. V. De sjeldne mineraler pa de norske granittiske pegmatittganger. *Norges Geologiske Undersokelse* **154**, 1-78.

BONAZZI, P. & MENCHETTI, S. (1994): Structural variations induced by heat treatment in allanite and REE-bearing piemontite. *Am. Mineral.* **79**, 1176-1184.

BONAZZI, P. & MENCHETTI, S. (1995): Monoclinic members of the epidote group: effects of the $Al \rightleftarrows Fe^{3+} \rightleftarrows Fe^{2+}$ substitution and the entry of REE^{3+}. *Mineral. Petrol.* **53**, 133-153.

DEER, W.A., HOWIE, R.A. & ZUSSMAN, J. (1986): *Rock-Forming Minerals.* **1B**. *Disilicates and Ring Silicates.* Longmans, London, U.K. (629).

EWING, R.C. (1987): The structure of the metamict state. *In* Second Int. Conf. on Natural Glasses (J. Konta, ed.). Charles University, Praha, Czech Republic (41-48).

EWING, R.C. (1994): The metamict state: 1993 – the centennial. *Nucl. Instr. Methods in Phys. Res.* **B91**, 22-29.

GEISLER, T., ZHANG, MING & SALJE, E.K.H. (2003): Recrystallization of almost fully amorphous zircon under hydrothermal conditions: an infrared spectroscopic study. *J. Nucl. Mater.* **320**, 280-291.

GRAHAM, J. & THORNBER, M.R. (1974): The crystal chemistry of complex niobium and tantalum oxides. IV. The metamict state. *Am. Mineral.* **59**, 1047-1050.

HOLLAND, T.J.B. & REDFERN, S.A.T. (1997): Unit cell refinement from powder diffraction data: the use of regression diagnostics. *Mineral. Mag.* **61**, 65-77.

JANECZEK, J. & EBY, R.K. (1993): Annealing of radiation damage in allanite and gadolinite. *Phys. Chem. Minerals* **19**, 343-356.

LIMA-DE-FARIA, J. (1958): Heat treatment of metamict euxenites, polymignites, yttrotantalites, samarskites and allanites. *Mineral. Mag.* **31**, 937-942.

MCEACHERN, S.J. & VAN BREEMEN, O. (1993): Age of deformation within the Central Metasedimentary Belt boundary thrust zone, southwest Grenville Orogen: constraints on the collision of the Mid-Proterozoic Elzevir terrane. *Can. J. Earth Sci.* **30**, 1155-1165.

MELGAREJO, J.C. & PROL-LEDESMA, R.M. (1999): Th and REE deposits in the Oaxaca Complex in southern Mexico. *In* Mineral Deposits: Processes to Processing (C.J. Stanley *et al.*, eds.). Proc. Fifth Biennial SGA Meeting, Tenth Quadrennial IAGOD Meeting. A.A. Balkema, Rotterdam, The Netherlands (389-392).

MEZGER, K., ESSENE, E.J., VAN DER PLUIJM, B.A. & HALLIDAY, A.N. (1993): U–Pb geochronology of the Grenville Orogen of Ontario and New York: constraints on ancient crustal tectonics. *Contrib. Mineral. Petrol.* **114**, 13-26.

MITCHELL, R.S. (1966): Virginia metamict minerals: allanite. *Southeastern Geol.* **7**, 183-195.

PANALYTICAL (2004): X'Pert High Score Plus, version 2.1. Panalytical, Almelo, The Netherlands.

PANCZER, W.D. (1987): *Minerals of Mexico.* Van Nostrand Reinhold Co., New York, N.Y. (459).

TOMAŠIĆ, N., GAJOVIĆ, A., BERMANEC, V., SU, D. S., RAJIĆ LINARIĆ, M., NTAFLOS, T. & SCHLÖGL, R. (2006): Recrystallization mechanisms of fergusonite from metamict mineral precursors. *Phys. Chem. Minerals* **33**, 145-159.

VANCE, E.R. & ROUTCLIFFE, P. (1976): Heat treatment of some metamict allanites. *Mineral. Mag.* **40**, 521-523.

WANG, L.M., EBY, R.K., JANECZEK, J. & EWING, R.C. (1991): In situ TEM study of ion-beam-induced amorphization of complex silicate structures. *Nucl. Instrum. Methods in Phys. Res.* **B59/60**, 395-400.

WEBER, W.J., EWING, R.C., CATLOW, C.R.A., DIAZ DE LA RUBIA, T., HOBBS, L.W., KINOSHITA, C., MATZKE, H., MOTTA, A.T., NASTASI, M., SALJE, E.K.H., VANCE, E.R. & ZINKLE, S.J. (1998): Radiation effects in crystalline ceramics for the immobilization of high-level nuclear waste and plutonium. *J. Mater. Res.* **13**, 1434-1484.

Received October 29, 2009, revised manuscript accepted May 28, 2010.